

Supporting Information

Adjustable coordination of a hybrid phosphine-phosphine oxide ligand
in luminescent Cu, Ag and Au complexes

*Thuy Minh Dau,^a Benjamin Darko Asamoah,^a Andrey Belyaev,^a Gomathy Chakkaradhari,^a Pipsa Hirva,^{*a} Janne Jänis,^a Elena V. Grachova,^b Sergey P. Tunik^b and Igor O. Koshevoy^{*a}*

[†] Department of Chemistry, University of Eastern Finland, Joensuu, 80101, Finland.

[§] St. Petersburg State University, 7/9 Universitetskaya nab., 199034, St. Petersburg, Russia.

E-mail: pipsa.hirva@uef.fi; igor.koshevoy@uef.fi

Table S1. Crystal data for **1–4**.

Table S2. Crystal data for **5–10**.

Table S3. Crystal data for **11, 12, 15, 16**.

Table S4–S7. Selected bond lengths and angles for complexes **1–12, 15, 16**.

Table S8. Electron density properties at the selected bond critical points (BCP) according to the QTAIM analysis of the mononuclear complexes **7, 10, 13** and **16**.

Table S9. Percentage contribution (%) of different fragments in the frontier MOs of singlet and triplet state complexes **7, 10, 13, 16**.

Figure S1. ESI mass spectra of **1–4**.

Figures S3–S4. 400 MHz ^1H – ^1H COSY NMR spectra of **1, 2, 4**.

Figure S5. Bond critical points and bond paths according to the QTAIM analysis in bimetallic Cu, Ag and Au compounds **1–4**.

Figure S6–S7. Molecular views of complexes **6–8, 10–12, 15, 16**.

Figure S8–S10. Normalized solid state excitation and emission spectra of **1–4, 7–16** at 77 K.

Figure S11. The appearance of the frontier MOs in the optimized singlet and triplet state in bimetallic compound **1**.

Table S1. Crystal data for **1–4**.

	1	2	3	4
Empirical formula	C ₉₀ H ₇₈ Cu ₂ F ₁₂ O ₄ P ₈	C ₉₄ H ₈₆ Ag ₂ F ₆ O ₁₀ P ₆ S ₂	C ₈₄ H ₆₆ Au ₂ F ₁₂ O ₂ P ₈	C ₈₄ H ₆₆ AuCuF ₁₂ O ₂ P ₈
FW	1826.36	1955.31	1977.07	1843.65
T (K)	120(2)	120(2)	120(2)	120(2)
λ (Å)	0.71073	0.71073	0.71073	0.71073
Cryst syst	Triclinic	Monoclinic	Monoclinic	Monoclinic
Space group	<i>P</i> 1	<i>P</i> 2 ₁ / <i>n</i>	<i>C</i> 2/ <i>c</i>	<i>P</i> 2 ₁ / <i>c</i>
<i>a</i> (Å)	13.4125(6)	14.1014(7)	32.139(2)	27.230(2)
<i>b</i> (Å)	13.7925(11)	13.3900(7)	15.1473(10)	16.1001(12)
<i>c</i> (Å)	13.9044(6)	23.1422(13)	22.6292(14)	23.2802(19)
α (deg)	97.099(3)	90	90	90
β (deg)	113.456(2)	101.235(2)	126.759(2)	114.689(6)
γ (deg)	109.776(3)	90	90	90
Volume (Å ³)	2118.8(2)	4285.9(4)	8825.9(10)	9273.3(13)
Z	1	2	4	4
ρ calc (Mg/m ³)	1.431	1.515	1.488	1.321
μ (mm ⁻¹)	0.730	0.691	3.534	2.012
F(000)	936	2000	3888	3688
Crystal size (mm ³)	0.224 x 0.096 x 0.080	0.099 x 0.065 x 0.019	0.202 x 0.074 x 0.070	0.511 x 0.289 x 0.192
θ range for data collection (deg.)	1.806 to 27.0	1.568 to 29.308	1.622 to 25.498	1.509 to 26.0
Index ranges	-17<=h<=17, -17<=k<=17, -17<=l<=17	-19<=h<=19, -18<=k<=17, -31<=l<=31	-38<=h<=37, -18<=k<=18, -22<=l<=27	-33<=h<=33, -19<=k<=19, -28<=l<=28
No.reflns.	39128	40813	39646	124399
Unique reflns.	9187	11331	8201	18218
Completeness to θ=25.242°	99.4 %	96.8 %	99.8 %	100.0 %
Absorption correction	Multi-scan	Numerical	Multi-scan	Numerical
GOOF (F ²)	1.052	1.014	1.042	1.044
R _{int}	0.0257	0.0523	0.0275	0.0556
R1 ^a (<i>I</i> ≥2σ)	0.0432	0.0505	0.0340	0.0441
wR2 ^b (<i>I</i> ≥2σ)	0.1112	0.1057	0.0876	0.1090
Largest diff. peak and hole (e.Å ⁻³)	1.060 and -1.152	1.273 and -1.064	4.885 and -2.589	2.865 and -1.334

^a RI = Σ||*F*_o| - |*F*_c||/Σ|*F*_o|. ^b wR2 = [Σ[w(*F*_o² - *F*_c²)²]/Σ[w(*F*_o²)²]]^{1/2}.

Table S2. Crystal data for **5–10**.

	5	6	7	8	9	10
Empirical formula	C ₄₂ H ₃₃ ClCuO P ₃	C ₄₂ H ₃₃ BrCu OP ₃	C ₄₃ H ₃₅ Cl ₂ CuI OP ₃	C ₄₅ H ₃₉ AgClO P ₃	C ₄₃ H ₃₅ AgBrC I ₂ OP ₃	C ₄₂ H ₃₃ AgIOP ₃
FW	745.59	790.04	921.97	847.99	919.29	881.36
T (K)	120(2)	120(2)	120(2)	120(2)	120(2)	120(2)
λ (Å)	0.71073	0.71073	0.71073	0.71073	0.71073	0.71073
Cryst syst	Triclinic	Monoclinic	Orthorhombic	Monoclinic	Monoclinic	Orthorhombic
Space group	<i>P</i> 1	<i>P</i> 2 ₁ / <i>n</i>	<i>P</i> 2 ₁ 2 ₁ 2 ₁	<i>P</i> 2 ₁ / <i>c</i>	<i>P</i> 2 ₁ / <i>n</i>	<i>Pna</i> 2 ₁
<i>a</i> (Å)	10.1924(3)	9.1856(3)	13.2014(10)	11.2147(10)	12.327(10)	19.311(2)
<i>b</i> (Å)	10.6291(3)	19.7157(6)	15.8615(12)	10.9485(6)	20.137(19)	18.4966(15)
<i>c</i> (Å)	18.1387(5)	19.6397(6)	18.2144(15)	32.358(2)	16.354(13)	10.3114(7)
α (deg)	99.7270(10)	90	90	90	90	90
β (deg)	97.9310(10)	93.3800(10)	90	93.236(7)	106.815(11)	90
γ (deg)	111.2170(10)	90	90	90	90	90
V (Å ³)	1762.63(9)	3550.57(19)	3814.0(5)	3966.8(5)	3886(6)	3683.1(6)
Z	2	4	4	4	4	4
ρ _{calc} (Mg/m ³)	1.405	1.478	1.606	1.447	1.571	1.589
μ (mm ⁻¹)	0.865	1.909	1.683	0.737	1.842	1.548
F(000)	768	1608	1848	1768	1848	1752
Crystal size (mm ³)	0.279 x 0.236 x 0.106	0.539 x 0.124 x 0.088	0.268 x 0.108 x 0.088	0.285 x 0.264 x 0.148	0.185 x 0.088 x 0.067	0.965 x 0.322 x 0.197
θ range for data collection (deg.)	1.167 to 25.499	1.465 to 30.042	1.905 to 32.646	1.261 to 25.049	1.648 to 24.997	1.524 to 31.996
No.reflns.	55770	65090	27206	47125	77940	121032
Unique reflns.	8510	10346	12883	7023	6843	12786
Completeness to θ=25.242°	100.0 %	99.7 %	99.9 %	100.0 %	100.0 %	99.8 %
Absorption correction	Multi-scan	Numerical	Numerical	Multi-scan	Multi-scan	Numerical
GOOD (F ²)	1.015	1.077	1.047	1.022	1.044	1.078
R _{int}	0.0939	0.0649	0.0419	0.0342	0.0435	0.0306
R1 ^a (<i>I</i> ≥ 2σ)	0.0419	0.0457	0.0373	0.0618	0.0239	0.0248
wR2 ^b (<i>I</i> ≥ 2σ)	0.0819	0.0837	0.0822	0.1434	0.0544	0.0601
Largest diff. peak and hole (e.Å ⁻³)	1.025 and -0.537	0.838 and -0.811	1.277 and -0.788	7.526 and -2.490	0.487 and -0.266	1.341 and -0.518

^a RI = Σ||*F*₀| - |*F*_c||/Σ|*F*₀|. ^b wR2 = [Σ[w(*F*₀² - *F*_c²)²]/Σ[w(*F*₀²)²]]^{1/2}.

Table S3. Crystal data for **11**, **12**, **15**, **16**.

	11	12	15	16
Empirical formula	C ₄₂ H ₃₃ ClCuP ₃	C ₄₂ H ₃₃ BrCuP ₃	C ₄₂ H ₃₃ AgBrP ₃	C ₄₂ H ₃₃ AgIP ₃
FW	729.59	774.04	818.36	865.36
T (K)	120(2)	120(2)	120(2)	120(2)
λ (Å)	0.71073	0.71073	0.71073	0.71073
Cryst syst	Monoclinic	Monoclinic	Monoclinic	Monoclinic
Space group	<i>P</i> 2 ₁ / <i>n</i>	<i>P</i> 2 ₁ / <i>n</i>	<i>P</i> 2 ₁ / <i>n</i>	<i>P</i> 2 ₁ / <i>c</i>
<i>a</i> (Å)	13.489(6)	13.4272(6)	13.5239(5)	12.3318(11)
<i>b</i> (Å)	18.443(8)	18.5516(8)	18.7050(7)	15.3248(16)
<i>c</i> (Å)	13.700(6)	13.7711(6)	13.8376(5)	19.1076(9)
α (deg)	90	90	90	90
β (deg)	96.614(6)	96.0870(10)	95.501(2)	95.457(6)
γ (deg)	90	90	90	90
V (Å ³)	3386(2)	3411.0(3)	3484.3(2)	3594.6(5)
Z	4	4	4	4
ρ_{calc} (Mg/m ³)	1.431	1.507	1.560	1.599
μ (mm ⁻¹)	0.897	1.983	1.893	1.583
F(000)	1504	1576	1648	1720
Crystal size (mm ³)	0.254 x 0.184 x 0.088	0.488 x 0.141 x 0.104	0.847 x 0.355 x 0.325	0.472 x 0.198 x 0.186
θ range for data collection (deg.)	1.860 to 27.999	1.848 to 31.538	1.836 to 44.043	1.706 to 27.999
No.reflns.	78004	83446	188706	116712
Unique reflns.	8167	11384	27289	8681
GOOF (F ²)	1.041	1.011	1.032	1.060
Completeness to $\theta=25.242^\circ$	100.0 %	100.0 %	100.0 %	100.0 %
Absorption correction	Multi-scan	Multi-scan	Numerical	Multi-scan
R _{int}	0.0259	0.0899	0.0395	0.0300
R1 ^a ($I \geq 2\sigma$)	0.0241	0.0435	0.0337	0.0212
wR2 ^b ($I \geq 2\sigma$)	0.0613	0.0751	0.0689	0.0576
Largest diff. peak and hole (e.Å ⁻³)	0.493 and -0.332	0.878 and -0.636	1.844 and -0.939	0.974 and -0.622

^a RI = $\Sigma ||F_o| - |F_c|| / \Sigma |F_o|$. ^b wR2 = $[\Sigma [w(F_o^2 - F_c^2)^2] / \Sigma [w(F_o^2)^2]]^{1/2}$.

Table S4. Selected bond lengths and angles for complexes **1–3**.

	1 (M = Cu)	2 (M = Ag)	3 (M = Au)
Bond lengths, Å			
M(1)–M(2/1')	3.2785(2)	4.4747(2)	4.4771(3)
P(1)–M(1)	2.2397(7)	2.4494(8)	2.309(1)
P(3)–M(1/2)	2.2199(7)	2.4343(8)	2.307(1)
O(1)–M(1)	2.1213(17)	2.457(2)	2.986(1)
O(1)–M(2/1')	2.1976(17)	2.885(1)	2.745(1)
O(1)–P(2)	1.521(2)	1.491(2)	1.494(4)
Bond angles, deg.			
P(1)–M(1)–P(3/1')	120.02(3)	131.77(3)	164.34(7)
P(3')–M(2)–P(3')	–	–	159.80(7)

Table S5. Selected bond lengths and angles for complex **4**.

4	
Bond lengths, Å	
Cu(1)–Au(1)	4.0052(2)
P(1)–Au(1)/P(6)–Au(1)	2.297(1)/ 2.297(1)
P(3)–Cu(1)/P(4)–Cu(1)	2.230(1)/ 2.223(1)
O(1)–Cu(1)/O(2)–Cu(1)	2.184(3)/ 2.163(3)
O(1)–Au(1)/O(2)–Au(1)	2.961(1)/ 2.938(1)
O(1)–P(2)/O(2)–P(5)	1.507(3)/ 1.506(3)
Bond angles, deg.	
P(3)–Cu(1)–P(4)	130.99(5)
P(1)–Au(1)–P(6)	167.04(4)

Table S6. Selected bond lengths and angles for complexes **5–10**.

	Bond lengths, Å			Bond angles, deg.	
	M–P	M–O	M–X	P–M–X	P(1)–M–P(3)
Cu(<i>P</i>³<i>O</i>)Cl (5)	2.2448(9)	2.293(2)	2.2422(9)	117.94(3)	116.08(3)
	2.2602(9)			119.41(3)	
6	2.2440(7)	2.381(2)	2.3705(4)	105.68(2)	137.15(3)
	2.2361(6)			117.01(2)	
7	2.2840(11)	2.174(2)	2.5688(5)	122.32(3);	115.59(4)
	2.2665(11)			120.59(3)	
8	2.6148(13)	2.536(3)	2.4472(13)	118.53(5)	112.65(4)
	2.4825(12)			128.79(5)	
9	2.492(2)	2.511(2)	2.5698(15)	122.71(4)	113.21(3)
	2.505(2)			123.99(4)	
10	2.5083(8)	2.647(3)	2.7130(3)	115.29(2)	115.66(3)
	2.5170(7)			127.23(2)	

Table S7. Selected bond lengths and angles for complexes **11, 12, 15, 16**.

	Bond lengths, Å		Bond angles, deg.	
	M–P	M–X	P–M–X	P(1)–M–P(3)
Cu(<i>P</i>³)Cl (11)	2.2954(7)	2.2748(7)	121.80(2)	115.423(15)
	2.2896(8)		120.24(3)	
	2.3038(10)		115.48(2)	
Cu(<i>P</i>³)Br (12)	2.2826(5)	2.3986(3)	121.963(16)	116.24(2)
	2.2831(6)		119.394(17)	
	2.2906(5)		114.817(17)	
Ag(<i>P</i>³)Br (15)	2.4750(3)	2.57221(14)	122.122(7)	112.267(9)
	2.5433(3)		123.115(7)	
	2.4908(3)		121.672(7)	
Ag(<i>P</i>³)I (16)	2.5460(5)	2.7050(2)	121.297(12)	118.760(16)
	2.6244(5)		133.911(11)	
	2.5069(5)		117.125(13)	

Table S8. Electron density properties at the selected bond critical points (BCP) according to the QTAIM analysis of the mononuclear complexes **7**, **10**, **13** and **16**.

complex	BCP	ρ (eÅ ⁻³)	V /G	E _{INT} (kJmol ⁻¹)	$\delta(A,B)$	q(M)
7	Cu(1)…O(1)	0.264	0.99	-62.3	0.25	0.396
	P(2)-O(1)	1.482	1.33	-847.8	0.85	
	Cu-P	0.499	1.36	-112.3	0.62	
	Cu-I	0.407	1.32	-80.7	0.76	
10	Ag(1)…O(1)	0.184	1.02	-36.0	0.18	0.281
	P(2)-O(1)	1.497	1.33	-864.7	0.87	
	Ag-P	0.432	1.32	-84.1	0.55	
	Ag-I	0.391	1.32	-71.7	0.84	
13	Cu(1)-P(2)	0.486	1.36	-106.5	0.55	0.309
	Cu-P	0.479	1.36	-104.2	0.60	
	Cu-I	0.386	1.30	-73.9	0.73	
16	Ag(1)-P(2)	0.361	1.29	-66.0	0.44	0.207
	Ag-P	0.420	1.32	-80.8	0.56	
	Ag-I	0.375	1.31	-67.4	0.80	

Table S9. Percentage contribution (%) of different fragments in the frontier MOs of singlet and triplet state complexes **7**, **10**, **13**, **16**.

MO	ϵ (eV)	M	P(1)	P(2)	P(3)	O(1)	I
7							
LUMO	-1.38	25	11	9	20	2	4
HOMO	-4.79	18	11	0	6	0	56
HSOMO	-2.77	13	10	18	6	27	6
SOMO	-5.68	31	20	1	7	3	20
13							
LUMO	-1.20	22	25	9	5		4
HOMO	-4.97	19	6	16	4		42
HSOMO	-2.62	19	9	13	9		10
SOMO	-5.13	19	13	15	15		15
10							
LUMO	-1.45	6	17	18	8	9	1
HOMO	-4.91	11	8	0	5	0	69
HSOMO	-2.82	3	8	24	9	13	6
SOMO	-5.47	21	22	2	9	5	21
16							
LUMO	-1.21	18	9	8	24		1
HOMO	-5.06	11	2	14	6		57
HSOMO	-2.70	17	3	22	10		1
SOMO	-4.93	15	13	19	16		13

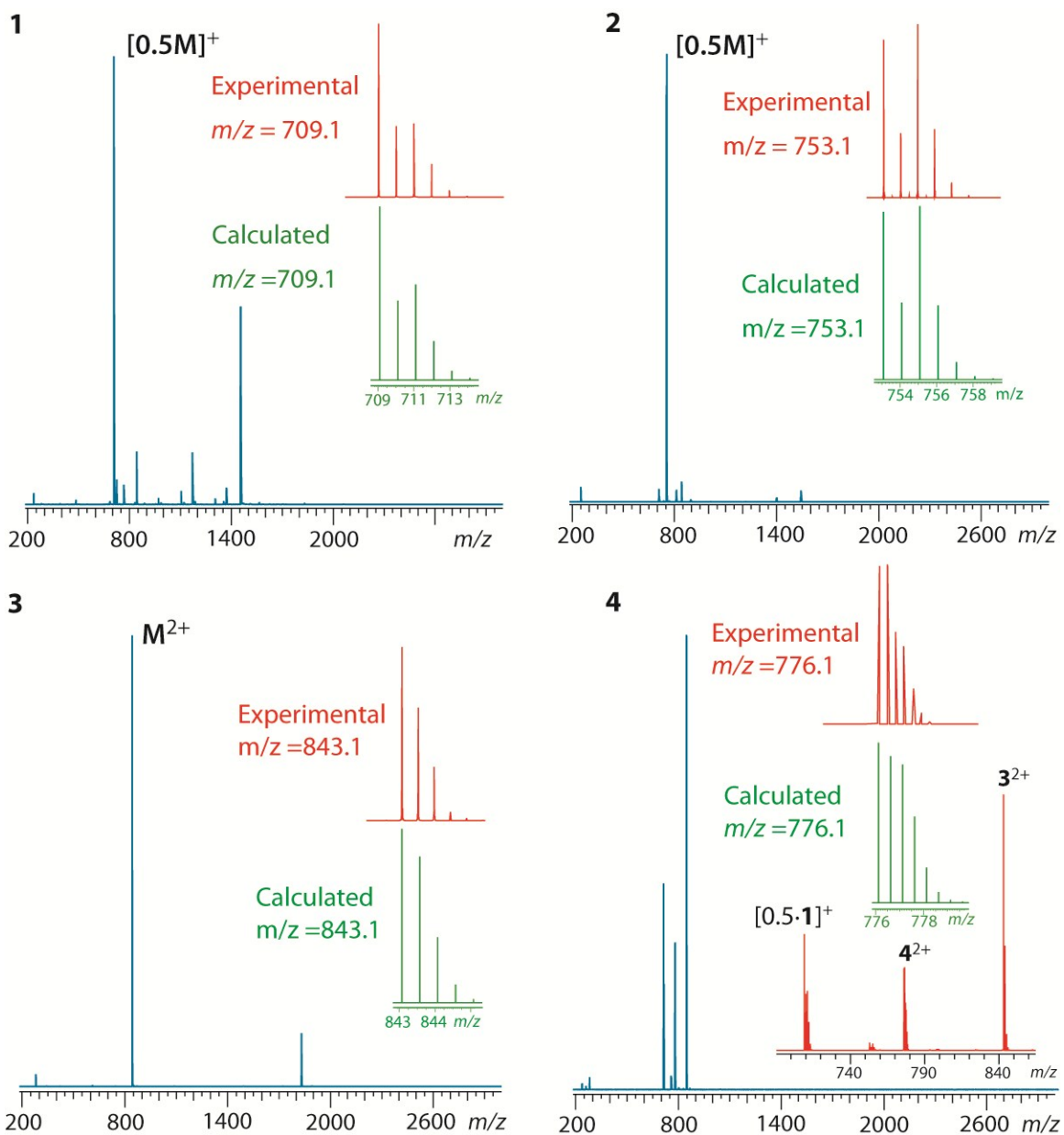


Figure S1. ESI mass spectra of **1–4**.

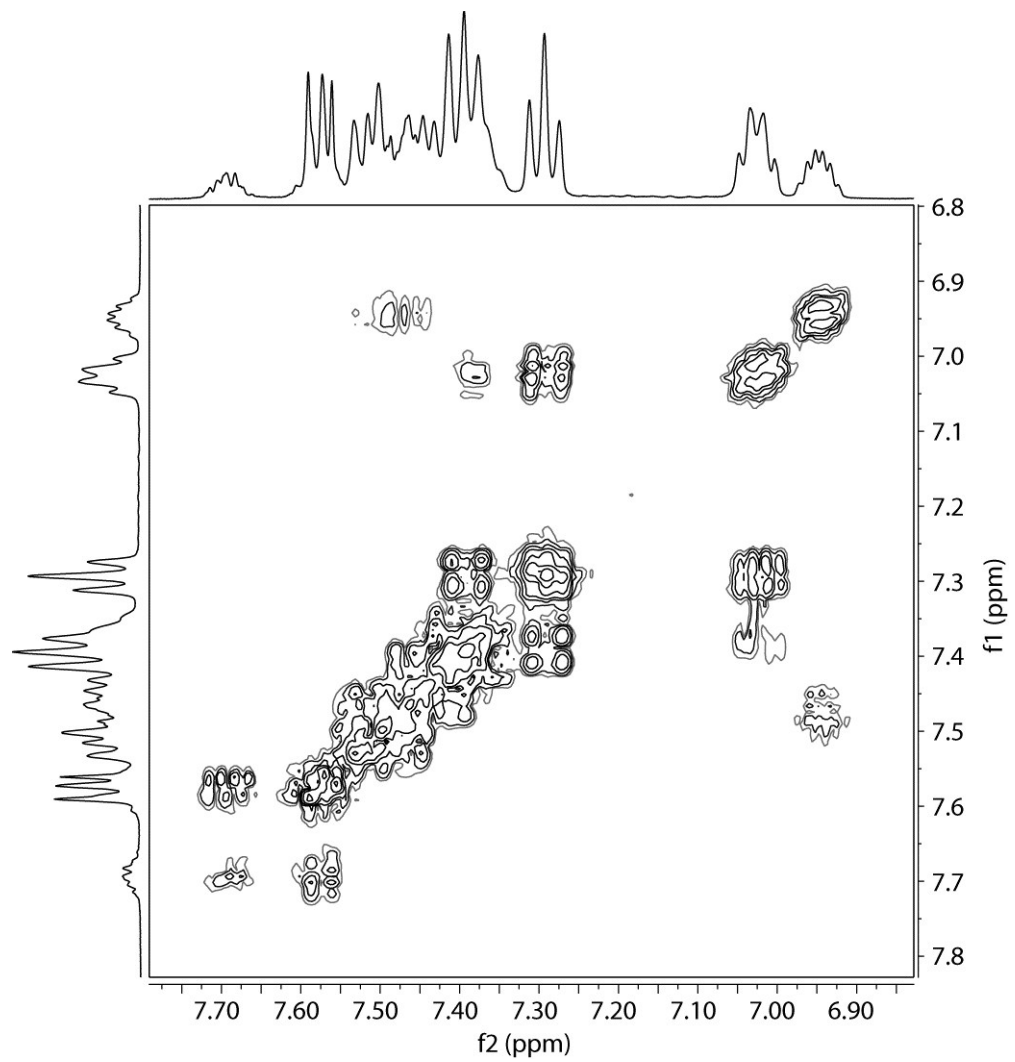


Figure S2. 400 MHz ^1H - ^1H COSY NMR spectrum of **1** ($\text{dmso}-d_6$, 298 K).

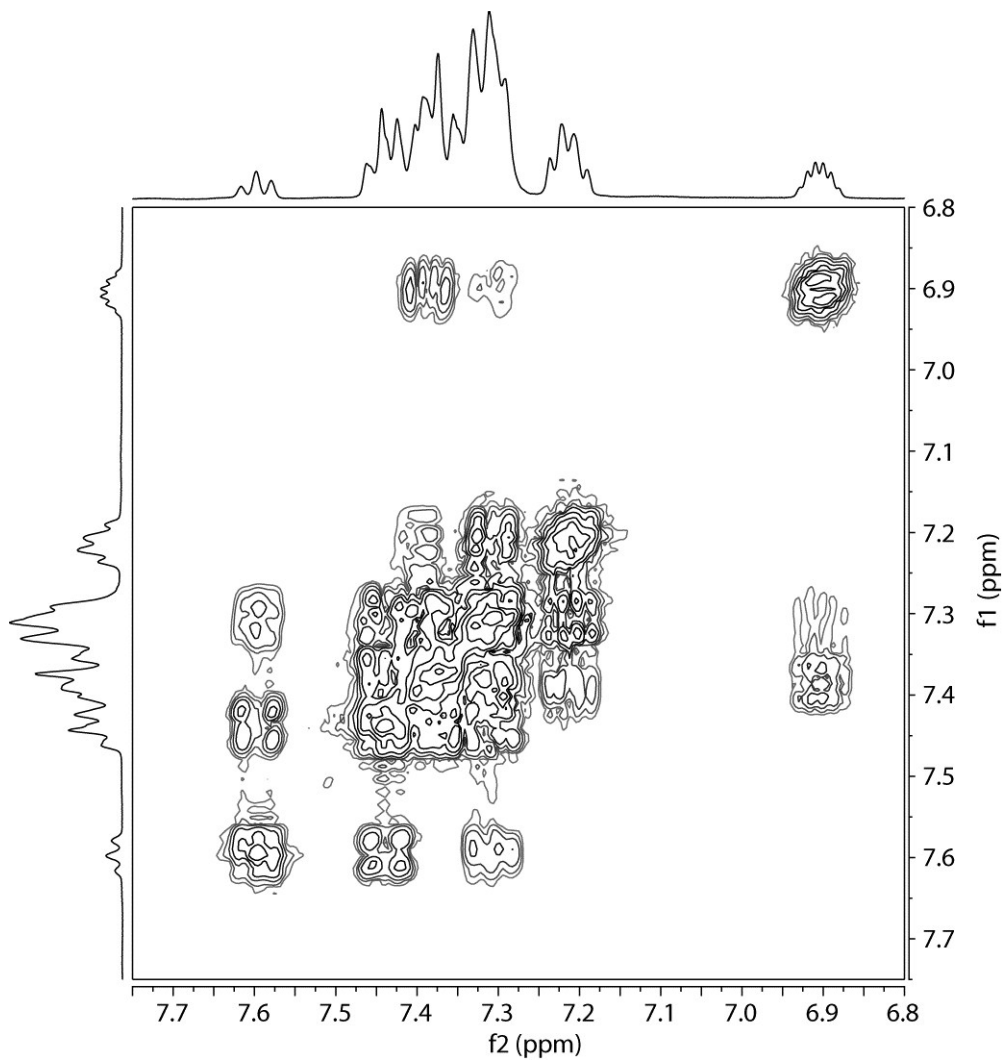


Figure S3. 400 MHz ¹H-¹H COSY NMR spectrum of **2** (dmso-*d*₆, 298 K).

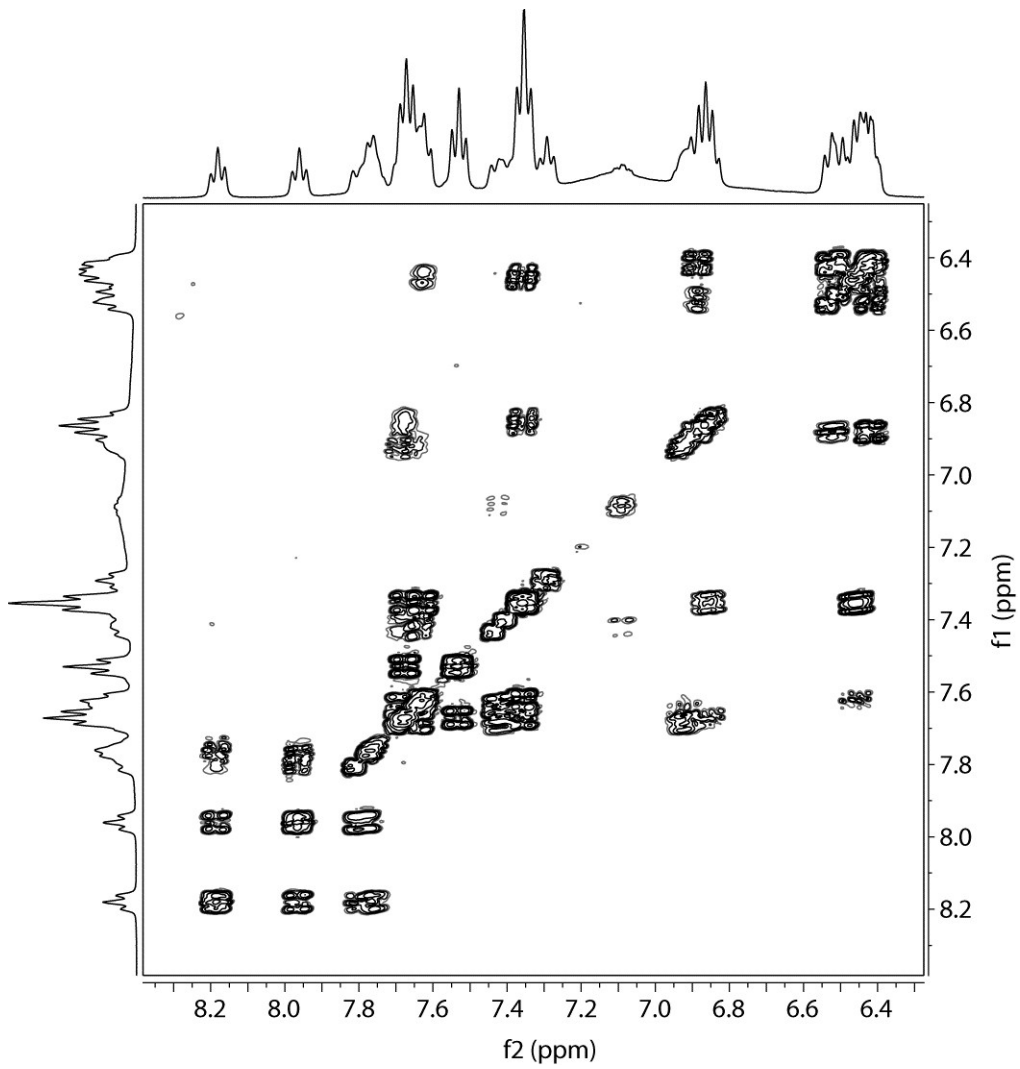


Figure S4. 400 MHz ^1H - ^1H COSY NMR spectrum of **4** ($\text{dmso}-\text{d}_6$, 298 K).

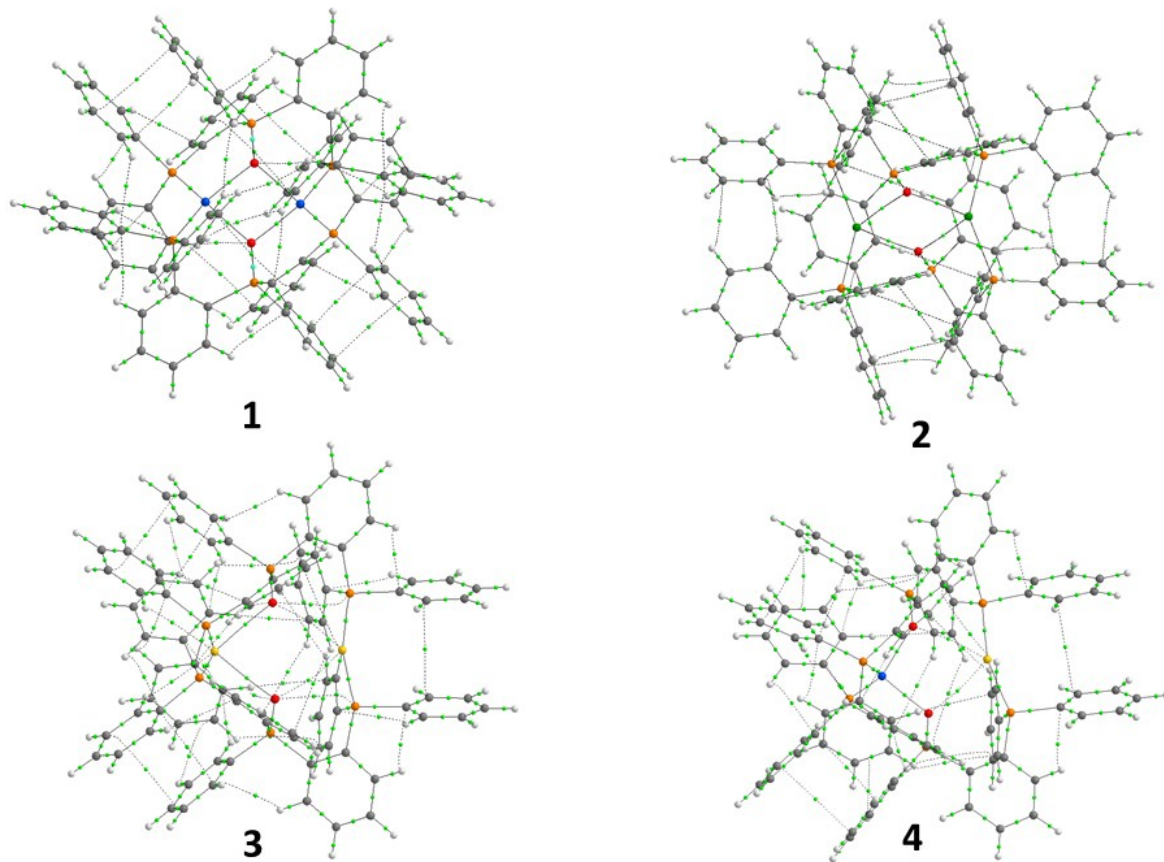


Figure S5. Bond critical points (BCPs, green dots) and bond paths according to the QTAIM analysis in bimetallic Cu, Ag and Au compounds **1–4**. Color coding: Cu = blue, Ag = green, Au = yellow, P = orange, O = red, C = gray, H = white.

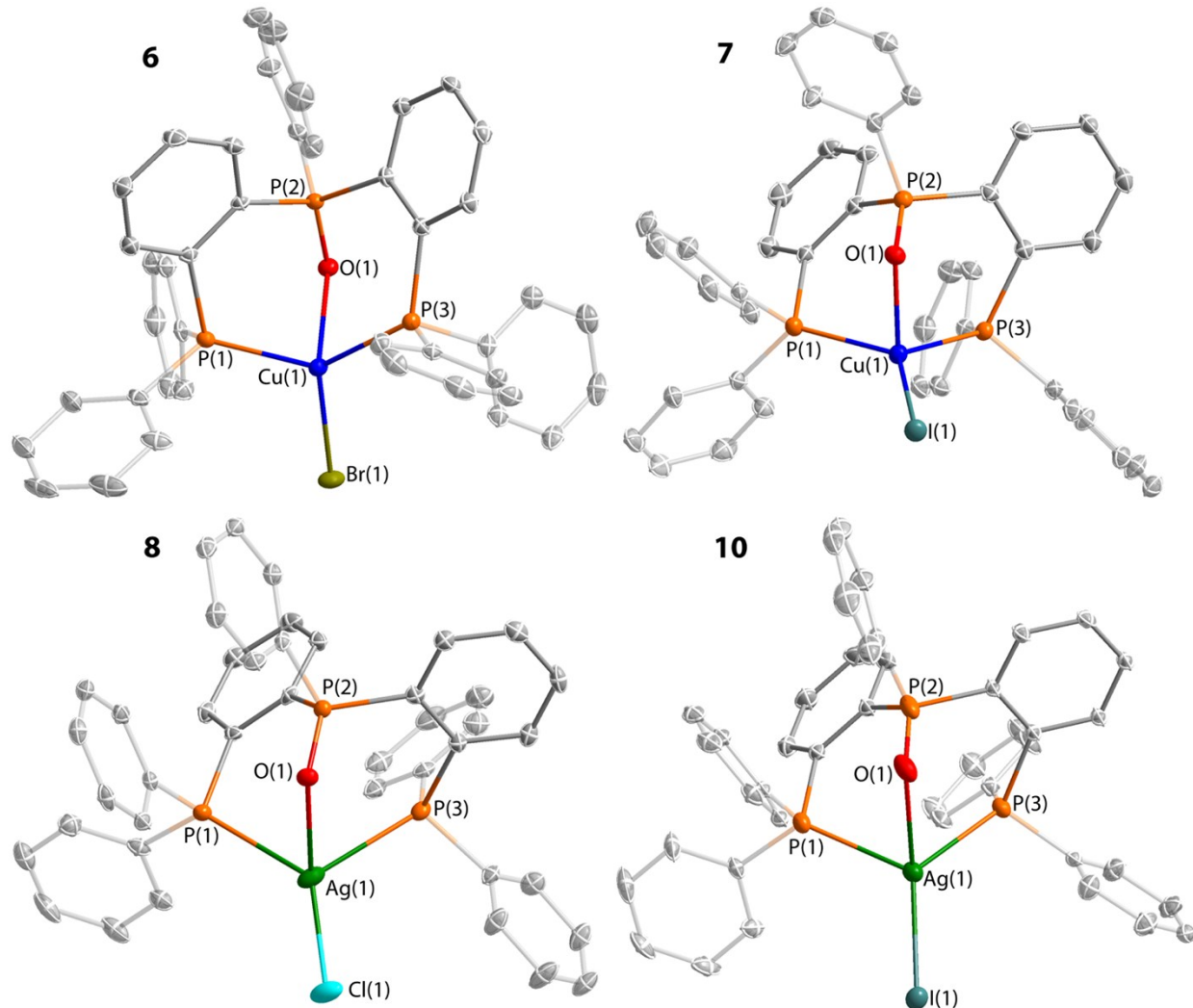


Figure S6. Molecular views of complexes **6–8, 10**. Thermal ellipsoids are shown at the 50% probability level. H atoms are omitted for clarity.

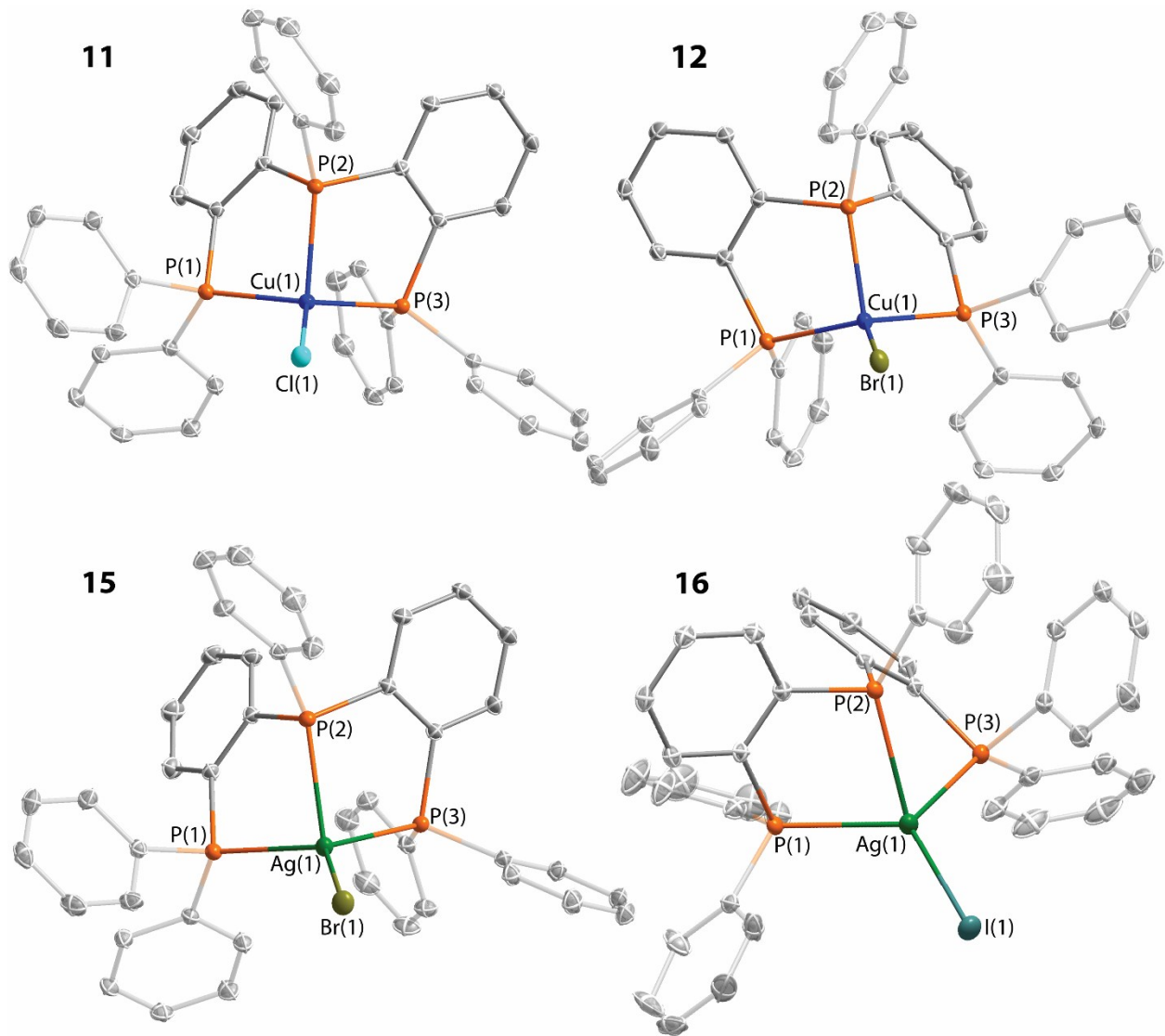


Figure S7. Molecular view of complexes **11**, **12**, **15**, **16**. Thermal ellipsoids are shown at the 50% probability level. H atoms are omitted for clarity.

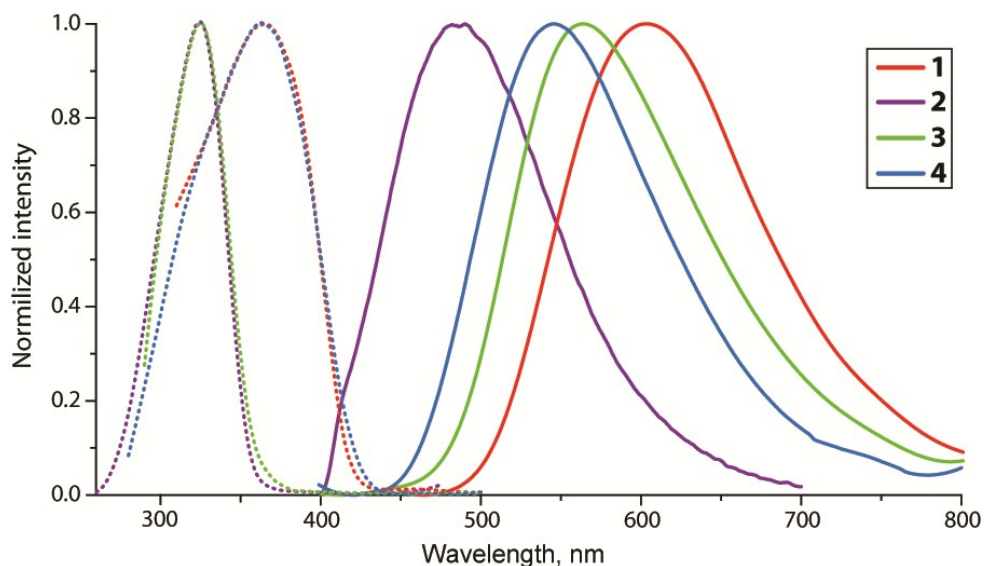


Figure S8. Normalized solid state excitation (dotted lines) and emission (solid lines) spectra of **1–4** at 77 K.

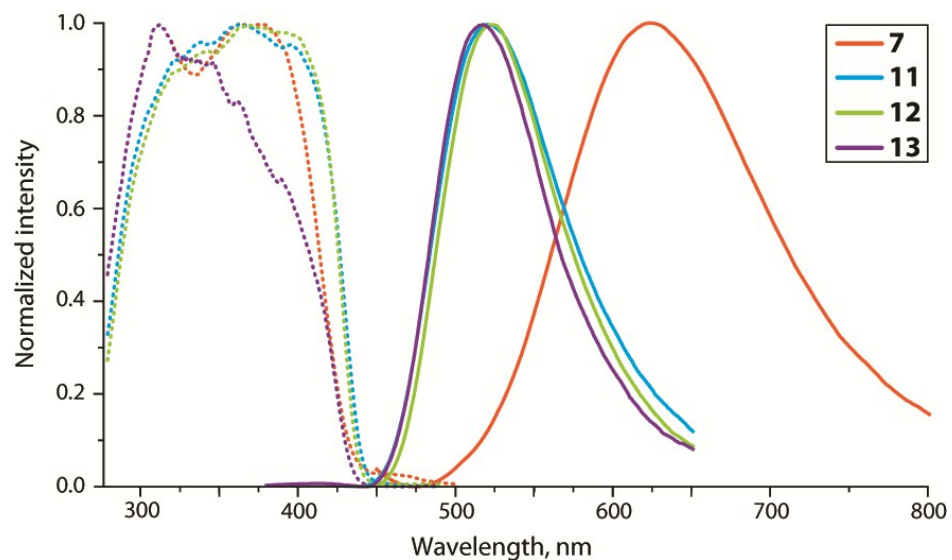


Figure S9. Normalized solid state excitation (dotted lines) and emission (solid lines) spectra of copper complexes **7** and **11–13** at 77 K.

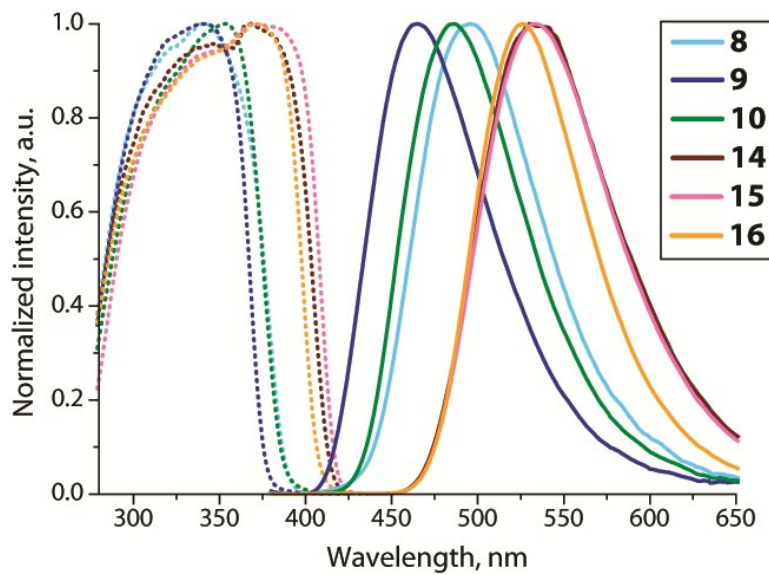


Figure S10. Normalized solid state excitation (dotted lines) and emission (solid lines) spectra of silver complexes **8–10** and **14–16** at 77 K.

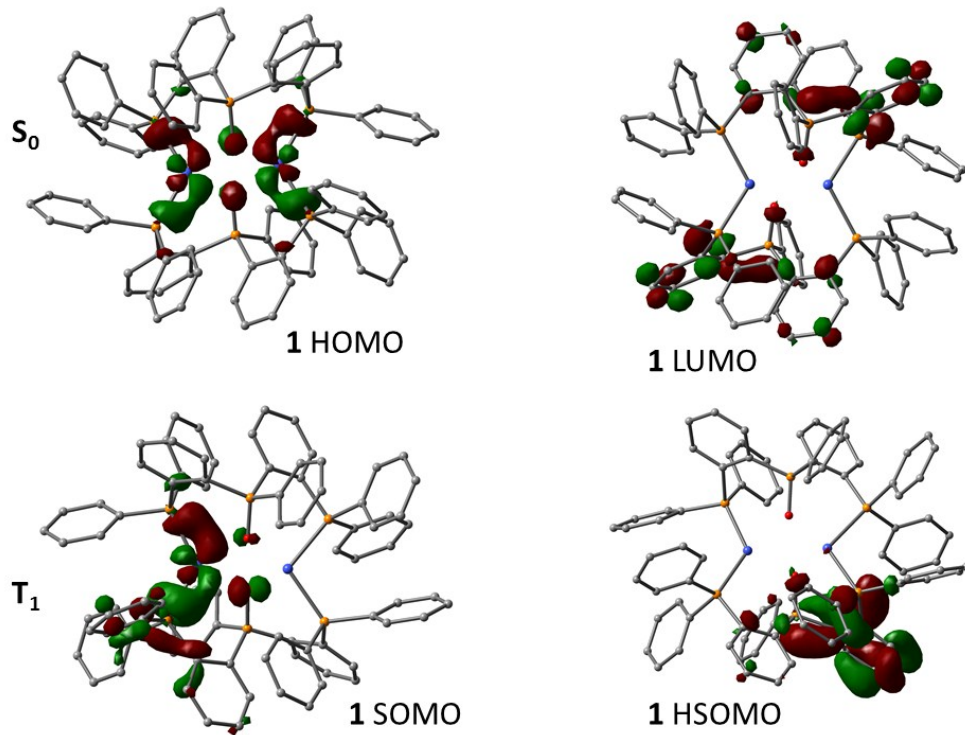


Figure S11. The appearance of the frontier MOs in the optimized singlet and triplet state in bimetallic compound **1**.